Proceedings of the 9th International Conference on Fluid Flow, Heat and Mass Transfer (FFHMT'22)
Niagara Falls, Canada – June 08-10, 2022
Paper No. 208
DOI: 10.11159/ffhmt22.208

Effect of Stack Position and Stack Length on the Performance of Thermoacoustic Engine

Yara Al Masalmeh[1], Ussama Ali[1], Md Islam[1], Isam Janajreh[1]
[1]Khalifa University of Science and Technology
Abu Dhabi, UAE
100059678@ku.ac.ae, ussama.ali@ku.ac.ae; didarul.islam@ku.ac.ae; isam.janajreh@ku.ac.ae

Abstract - In this paper, the influence of the stack length and stack position on the performance of the thermoacoustic engine is numerically investigated. In the thermoacoustic engine (TAE), thermal energy is converted into acoustic energy which can be utilized for various applications. Here, two stack lengths and five stack positions are used to study their effect on the parameters of the developed acoustic wave. The two stack sizes are 5% and 15% of the length of the resonator tube, whereas the stack centre position is varied between 10% to 50% of the resonator length. The results are given in terms of the pressure, axial velocity, and frequency of the acoustic wave. These quantities are observed at three different locations in the resonator tube, i.e., sensor 1, 2, and 3. The results indicated that longer stack produced the sound wave with higher intensity and higher frequency as compared to the shorter stack. Moving the stack away from the closed end of the resonator increased the frequency of the wave, whereas the pressure and velocity increased until a maximum peak was reached, and then started to decrease.

Keywords**:** Thermoacoustic engine; Stack design; Acoustic energy, Heat to sound, CFD; High Fidelity Flow

1. Introduction

The conventional energy systems, such as, the internal combustion engines and the vapor compression refrigerators pose a serious threat to the environment due to their harmful emissions [1, 2]. Thermoacoustic engine (TAE) uses thermal energy from a heat source to produce acoustic work [3], while the thermoacoustic refrigerator (TAR) utilizes the acoustic energy to obtain a temperature gradient [4]. Unlike conventional engines and refrigerators which require moving parts, maintenance, and hazardous refrigerants [5], thermoacoustic engines use environmentally friendly fluids, have no moving parts which reduces maintenance needs, and have low costs. Thermoacoustic devices can be classified as a green technology since they can utilize waste heat [6] or renewable sources as the thermal energy input. Thermoacoustic devices consist of three main components: the stack, hot and cold heat exchangers, and the resonator tube. The stack is the main component of any thermoacoustic device. The thermoacoustic stack is a porous solid material that allows for heat transfer between the fluid and the plates of the stack [7]. The thermal contact between the stack and the working fluid in the standing wave should be imperfect. It should not be too weak that no heat transfer happens between the stack and the working fluid, nor too strong where the working fluid's viscous properties will stand in the way of the oscillation of the fluid [8].

Despite the potential these devices hold, their low efficiencies stand in the way of their commercialization. When compared to other conventional methods for energy production and refrigeration, thermoacoustic devices have considerably lower efficiencies and coefficients of performance. This drawback led many researchers to investigate thermoacoustic devices both experimentally and numerically to come up with optimum design parameters. Wantha [9] conducted an experimental investigation on the influence of stack geometry on the cold side temperature of a TAR. Between the spiral stack, the circular pore stack, and the pin array stack, the pin array stack yielded the lowest cold temperature. However, their work suggested the use of the spiral stack due to easier manufacturing. The stack position was mentioned in the work of Kajurek and Rusowicz [10], where they experimentally investigated the performance of a thermoacoustic device. In their work they concluded that a wrong stack location will worsen the performance, however their work did not provide a recommended stack position.

The geometry of the resonator is also an area of investigation for the researchers in this area. Agustina et al. [11] concluded in their experimental investigation, that the cylindrical resonator achieved the lowest temperature gradient of 7.5°C when compared with the tapered and squared resonators. The influence of the resonator's length and diameter was

covered by Ghazali et al. [12]. Their experimental results concluded that increasing the diameter of the resonator gave a higher temperature gradient. They suggested that the higher temperature gradient was due to the increase in the number of plates that comes with the increase of diameter. Their work also concluded that the resonator's length does not affect the performance that much.

Apart from experimental work done in the thermoacoustic area, many numerical investigations have been conducted to optimize the performance of these devices. Yu et al. [13] used Ansys/Fluent to simulate a 300 Hz standing wave engine of an already existing experimental engine. Their work aimed at modeling the experimental engine with similar conditions to achieve fair comparison of results. Their findings in resonant frequency, onset temperature and pressure amplitude were a good match to the experimental data. Qiu et al. [14] numerically proved that the stack plate spacing plays an important part in the performance of TAR. Their results showed that the optimum stack plate spacing is 2.6-2.7 times δ_k, where δ_k is the thermal penetration depth. The thermal penetration depth is the distance surrounding the stack plate where thermoacoustic effects are present [4]. This finding was also supported by Nouh et al. [15] where their numerical study concluded that the optimal stack spacing was $2.4\delta_k$.

The literature shows that CFD can be a great tool to investigate thermoacoustic systems further. Many different parameters come in the picture when designing and optimizing the thermoacoustic device. While the literature covers many aspects of this technology, there is still a need for clearer guidelines and design specs for obtaining a high efficiency thermoacoustic device. This study highlights the importance of the stack length and position in designing and optimizing the thermoacoustic engine.

2. Methodology

The numerical analysis is carried out in Ansys/Fluent. Figure 1 shows the computational domain. The resonator tube is closed at one end and open at the other end to produce the travelling wave. The length (L) of the resonator tube is 45cm with a radius of 6.75mm and TAE stack is housed inside it. The top and left walls are prescribed with no-slip condition and with zero heat flux. The walls of the stack are also provided with no-slip condition. The bottom wall is provided with axisymmetric condition so that the computational domain represents only one-half section of the full circular tube. The left end of the TAE stack is heated at 1000K temperature, and the cold end is maintained at room temperature of 300K. The horizontal walls of the stack are imposed with the temperature gradient of 1000K to 300K. The domain is fitted with structured mesh with fine spacing near the walls. The time step of 1×10^{-5} second is chosen to satisfy the condition of CFL number ≤ 1. The numerical model solves the Navier-Stokes and the energy equations which represents the conservation laws of mass, momentum, and energy. The governing equations are given in Table 1. Air is used as the working fluid with density subjected to ideal gas law. The *k-ε* turbulence model is used to account for turbulence and to allow for the development of acoustic wave. The position of the TAE stack and its length is varied to observe the changes in the output parameters, i.e., pressure, axial velocity, and frequency of the developed acoustic wave. Two stack lengths of 5% of L and 15% of L are used. Each stack is placed at five different positions, i.e., 10% - 50% of the resonator length.

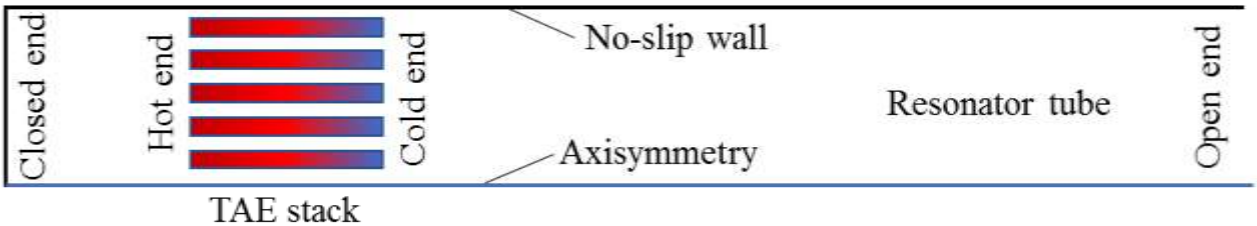

Fig. 1: The computational domain with the stack

Table 1: The governing equations

Conservation of mass	$$\frac{\partial(\rho_f)}{\partial t}+\frac{1}{r}\frac{\partial(r\rho_f v_f)}{\partial r}+\frac{\partial(\rho_f v_x)}{\partial x}$$ where ρ and v are the density and velocity, respectively. The radial and axial coordinates are represented by r and x. Time is represented by t. The subscript f means fluid.
Conservation of momentum	$$\frac{\partial(\rho_f \vec{v})}{\partial t}+\nabla.(\rho_f \vec{v}\vec{v})=-\nabla p+\nabla.(\tau)$$ where p and τ are the pressure and stress tensor, respectively.
Conservation of energy for the fluid	$$\frac{\partial(\rho_f E)}{\partial t}+\nabla.(\vec{v}(\rho_f E+p))=\nabla.[\hat{k}\nabla T+(\tau.\vec{v})]$$ where E, k, and T represent the internal energy, thermal conductivity, and temperature, respectively.
Ideal gas law	$$p=\rho RT$$ where R is the gas constant.
Conservation of energy for the solid part of the stack	$$\rho_s C_s\frac{\partial T_s}{\partial t}=\nabla.(K\nabla T_s)$$ where C is the heat capacity. The subscript s is for solid.

The thermal penetration depth (δ_k) and the viscous penetration depth (δ_v) play a very important role in the working of the thermoacoustic engine. These depths define how far the heat and momentum can diffuse, respectively, and are of immense importance in the design of the stack. Equation 1 and Equation 2 show the mathematical representation of these lengths:

$$\delta_k=\sqrt{\frac{2k}{\rho c_p \omega}} \tag{1}$$

$$\delta_v=\sqrt{\frac{2\mu}{\rho\omega}} \tag{2}$$

where, k is the thermal conductivity, ρ is the density, c_p is the heat capacity, and μ is the viscosity of the working gas. The values of these parameters are given is Table 2. The ω is the angular frequency and is represented as: $\omega = 2\pi f$, where f (Hz) is the frequency of the developed acoustic wave. For a standing wave thermoacoustic engine, the wavelength (λ) of the acoustic wave is 4 times the length of the resonator. Therefore, the theoretical frequency is calculated by Equation 3:

$$f=\frac{c}{\lambda}=\frac{c}{4L} \tag{3}$$

where, c is the speed of sound in the medium.

For successful working of TAE, an imperfect thermal contact is required between the working gas and the stack plates. This condition is fulfilled when the spacing between the stack plates is a few times of the thermal penetration depth. In this analysis, the distance between the stack plates is set to be 3.3 times δ_k.

Table 2: Properties of air

Parameter	Symbol	Value	Unit
Density	ρ	Ideal gas law	kg/m^3
Specific heat capacity	c_p	1.006×10^3	J/kgK
Thermal conductivity	k	2.42×10^2	W/mK
Dynamic viscosity	μ	1.79×10^{-5}	kg/ms
Viscous penetration depth	δ_v	1.59×10^{-4}	m
Thermal penetration depth	δ_k	1.84×10^{-4}	m

3. Results

Figure 2 shows the results represented in terms of the rms values of pressure and axial velocity of the acoustic wave. Sensor 1 and sensor 2 are placed at 1cm and 2cm from the cold end of the stack, respectively. While sensor 3 is placed at the exit of the resonator tube. The results show that the maximum pressure is observed at sensor 1 location while the velocity is minimum here. Keeping the stack fixed at one position, the pressure of the acoustic wave decreases as we go along the resonator tube while its velocity increases. This confirms the development of the standing wave as there is a pressure node at the exit of the tube and the velocity anti-node. The maximum pressure (9.8kPa) and maximum velocity (25.5 m/s) for short stack is observed at sensor 1 and 3, respectively, when the stack is placed at a location 20%L from the closed end. While the maximum values for the long stack (10.5kPa and 29.5 m/s) are observed with the stack position at 30%L from the closed end. The longer stack resulted in producing the acoustic wave with 8% higher pressure and 15% higher axial velocity than the shorter stack. This can be attributed to the fact that a longer stack will allow for more fluid particles to interact with the plates of the stack, thereby resulting in the acoustic wave with higher intensity.

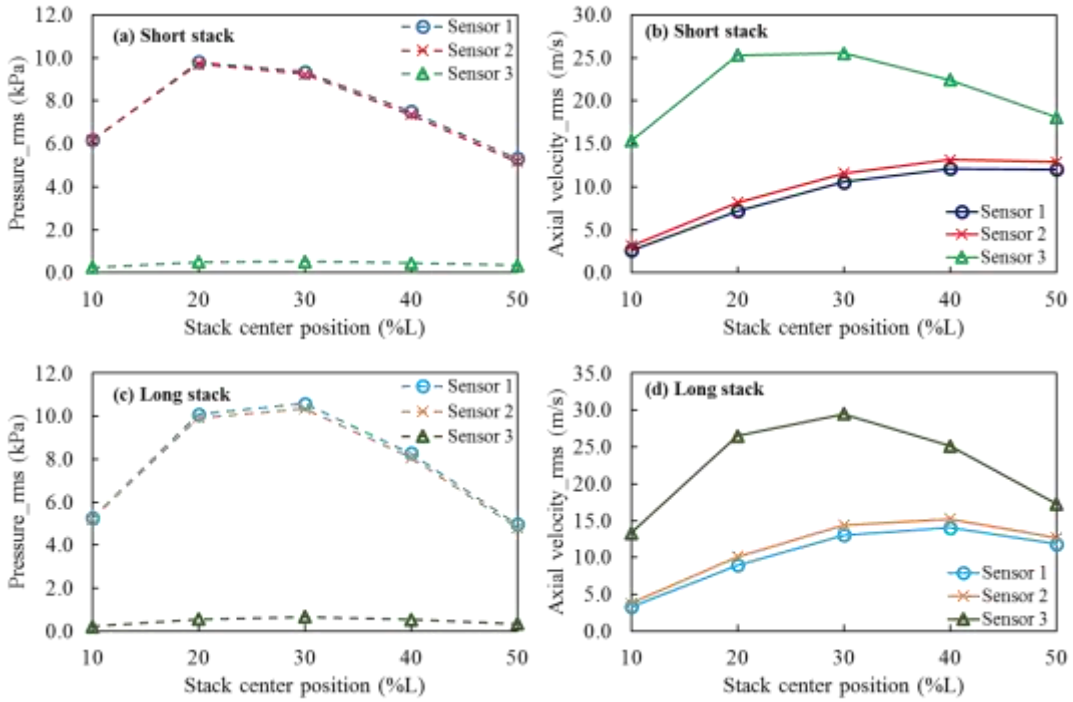

Fig. 2: rms of pressure and axial velocity for short and long stack with varying position of stack. The pressure plots are shown in dashed lines (--), while the velocity plots are shown in solid lines (—)

Figure 3 shows the pressure and axial velocity rms values for short and long stack at sensor 2 location. It is observed that the maximum pressure occurs when the short stack is placed at 20%L and the long stack placed at 30%L. While the maximum velocity for both the stacks is observed with stack position at 40%L. Therefore, the position and the length of the stack play an important role in the development of the acoustic wave. Figure 4 shows the frequency of the developed acoustic wave for each case. It is observed that the stack length as well as the stack position affects the frequency of the wave. The longer stack produces acoustic wave with higher frequency as compared to the shorter stack. Also, moving the stack away from the closed end of the resonator increases the frequency of the acoustic wave.

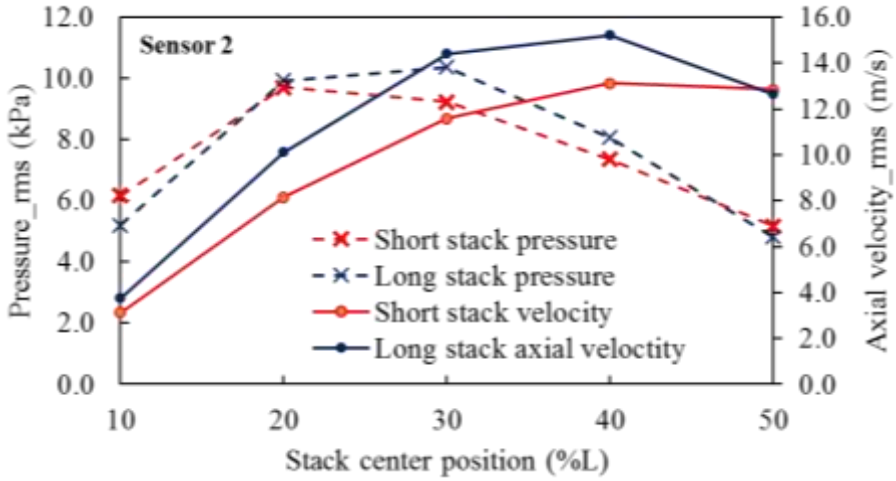

Fig. 3: rms of pressure and axial velocity for short and long stack with varying centre position. The readings are taken at sensor 2 location

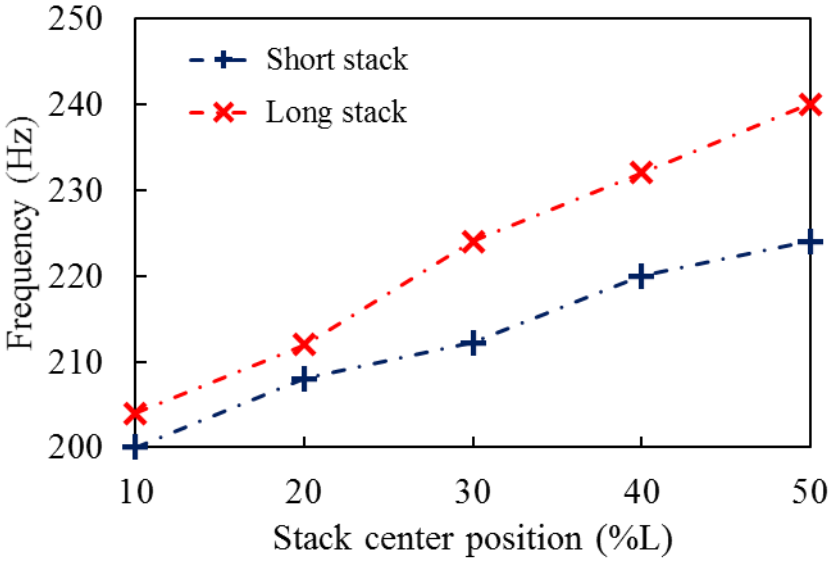

Fig. 4: Frequency of the developed acoustic wave using short and long stack as a function of the stack position

4. Conclusion

The effect of stack length and stack position, inside the resonator tube of a thermoacoustic engine, on the parameters the acoustic wave were numerically studied in this work. The results showed that both these variables affect the of the TAE. The longer stack performed better with 8% higher pressure and 15% higher axial velocity than the shorter Moving the stack towards the open end of the resonator resulted in increase in pressure and velocity up till 20%-30% of (depending upon the stack size) while further moving it decreased both the pressure and velocity. The frequency for both the stack sizes increased roughly in a linear manner while moving the stack towards the open end of resonator.

References

[1] A. Rai and S. A. Tassou, "Environmental impacts of vapour compression and cryogenic transport refrigeration technologies for temperature controlled food distribution," *Energy Conversion and Management*, vol. 150, pp. 914–923, 2017.

[2] O. A. Towoju and F. A. Ishola, "A case for the internal combustion engine powered vehicle," *Energy Reports*, vol. 6, pp. 315–321, 2020.

[3] P. H. Ceperley, "A pistonless Stirling engine—the traveling wave heat engine," *The Journal of the Acoustical Society of America*, vol. 66, no. 5, pp. 1508–1513, 1979.

[4] N. M. Hariharan, P. Sivashanmugam, & S. Kasthurirengan, "Influence of stack geometry and resonator length on the performance of thermoacoustic engine," *Applied Acoustics*, *73*(10), 1052–1058, 2012.

[5] M. E. Tijani and S. Spoelstra, "A high performance thermoacoustic engine," *Journal of Applied Physics*, vol. 110, no. 9, p. 093519, 2011.

[6] J. Zhou, X. Wang, M. Karlsson, and M. Abom, "Designing thermoacoustic engines for automotive exhaust waste heat recovery," *SAE Technical Paper Series*, 2021.

[7] A. J. Jaworski and X. Mao, "Development of thermoacoustic devices for power generation and refrigeration," *Proceedings of the Institution of Mechanical Engineers, Part A: Journal of Power and Energy*, vol. 227, no. 7, pp. 762–782, 2013.

[8] I. Setiawan, A. B. Utomo, M. Katsuta, & M. Nohtomi, "Experimental study on the influence of the porosity of parallel plate stack on the temperature decrease of a thermoacoustic refrigerator," *Journal of Physics: Conference Series*, 423, 2013.

[9] C. Wantha, "The impact of stack geometry and mean pressure on cold end temperature of stack in thermoacoustic refrigeration systems," *Heat and Mass Transfer*, *54*(7), 2153–2161, 2018.

[10] J. Kajurek & A. Rusowicz, "Performance analysis of the thermoacoustic refrigerator with the standing wave and air as a working fluid," *E3S Web of Conferences*, 44, 2018.

[11] D. Agustina, A. Sabri, S. Purnama, "Experimental investigation on the effect of resonator shapes on the temperature characteristic of thermoacoustic cooling device," *IOP Conference Series: Materials Science and Engineering*, 539, 2019.

[12] N. Mohd-Ghazali, A. D. Ghazali, I. S. Ali, M. A. Rahman, "Geometry effects on cooling in a standing wave cylindrical thermoacoustic resonator," AIP Conference Proceedings 1440, 1320, 2012.

[13] G. Yu, W. Dai, and E. Luo, "CFD simulation of a 300Hz thermoacoustic standing wave engine," *Cryogenics*, vol. 50, no. 9, pp. 615–622, 2010.

[14] L. M. Qiu, B. H. Lai, Y. F. Li, D. M. Sun, "Numerical simulation of the onset characteristics in a standing wave thermoacoustic engine based on thermodynamic analysis," *International Journal of Heat and Mass Transfer*, *55*(7-8), 2200–2203, 2012.

[15] M. A. Nouh, N. M. Arafa, E. Abdel-Rahman, "Stack parameters effect on the performance of anharmonic resonator thermoacoustic heat engine," *Archive of Mechanical Engineering*, 61(1), 115–127, 2014.